

# Late internal shock model for bright X-ray flares in Gamma-ray Burst afterglows and GRB 011121

Y. Z. Fan<sup>1,2,3\*</sup> and D. M. Wei<sup>1,2</sup> \*

<sup>1</sup>Purple Mountain Observatory, Chinese Academy of Science, Nanjing 210008, China

<sup>2</sup>National Astronomical Observatories, Chinese Academy of Sciences, Beijing 100012, China

<sup>3</sup>Dept. of Physics, University of Nevada, Las Vegas, NV 89154, USA.

Accepted ..... Received .....; in original form .....

## ABSTRACT

We explore two possible models which might give rise to bright X-ray flares in GRBs afterglows. One is an external forward-reverse shock model, in which the shock parameters of forward/reverse shocks are taken to be quite different. The other is a so called “late internal shock model”, which requires a refreshed unsteady relativistic outflow generated after the prompt  $\gamma$ -ray emission. In the forward-reverse shock model, after the time  $t_{\times}$  at which the RS crosses the ejecta, the flux declines more slowly than  $(t_{\oplus}/t_{\times})^{-(2+\beta)}$ , where  $t_{\oplus}$  denotes the observer’s time and  $\beta$  is the spectral index of the X-ray emission. In the “late internal shock model”, decaying slopes much steeper than  $(t_{\oplus}/t_{e,\oplus})^{-(2+\beta)}$  are possible if the central engine shuts down after  $t_{e,\oplus}$  and the observed variability timescale of the X-ray flare is much shorter than  $t_{e,\oplus}$ .

The sharp decline of the X-ray flares detected in GRB 011121, XRF 050406, GRB 050502b, and GRB 050730 rules out the external forward-reverse shock model directly and favors the “late internal shock model”. These X-ray flares could thus hint that the central engine operates again and a new unsteady relativistic outflow is generated just a few minutes after the intrinsic hard burst.

**Key words:** Gamma Rays: bursts–ISM: jets and outflows–radiation mechanisms: nonthermal–X-rays: general

## 1 INTRODUCTION

GRB 011121 was simultaneously detected by *BeppoSAX* GRBM and WFC (Piro 2001), and the fluence in the 2–700 keV range corresponds to an isotropic energy of  $2.8 \times 10^{52}$  ergs at the redshift of  $z = 0.36$  (Infante et al. 2001). This burst was born in a stellar wind (Price et al. 2002; Greiner et al. 2003) and a supernova bump was detected in the late optical afterglow (Bloom et al. 2002; Garnavich et al. 2003). Its very early X-ray light curve, which has not been published until quite recently, is characterized by the presence of two flares (Piro 2005, hereafter P05). In the first one, which is also the strongest of the two, the observed flux  $F$  rises and decays very steeply:  $F \propto t_{\oplus}^{10}$  for  $239 \text{ s} < t_{\oplus} < 270 \text{ s}$  and  $F \propto t_{\oplus}^{-7}$  for  $270 \text{ s} < t_{\oplus} < 400 \text{ s}$ , where  $t_{\oplus}$  is the observer’s time<sup>1</sup>. Such a peculiar flare in the early X-ray lightcurve of

GRBs has not been predicted before. P05 suggested that the X-ray flare represents the beginning of the afterglow.

In this Letter we explore two alternative models which might give rise to very early X-ray flare in GRB afterglows (§2): a forward-reverse shock model (§2.1) and a “late internal shock model” (§2.2). We compare the available data with the predictions of those models in §3 and summarize our results in §4, with some discussion.

## 2 POSSIBLE MODELS

### 2.1 The external forward-reverse shock model

The external forward-reverse shock model has been widely accepted on interpreting the early IR/optical flashes of GRB 990123, GRB 021211 and GRB 041219a (For observations, see: Akerlof et al. 1999; Fox et al. 2003; Li et al. 2003; Blake et al. 2005. For theoretical modeling, see: Sari & Piran 1999; Mészáros & Rees 1999; Wei 2003; Kumar & Panaitescu 2003; Fan, Zhang & Wei 2005). Synchrotron radiation from the reverse shock (RS) and the forward shock (FS) usually peaks in the infrared-to-optical and ultraviolet-to-soft X-ray bands, respectively. Thus, the RS emission component

\* E-mail: yzfan@pmo.ac.cn(YZF); dmwei@pmo.ac.cn(DMW)

<sup>1</sup> During our revision, bright X-ray flares peaking a few minutes after XRF 050406, GRB 050502b and GRB 050730 have been reported (Burrows et al. 2005; Starling et al. 2005). Sharp rise and fall are also evident in these events.

is not dominant in the X-ray band. The synchrotron self-Compton (SSC) scattering effect of the RS radiation has also been considered by different authors, but no strong X-ray emission is found to be expected (Wang, Dai & Lu 2001) except in some carefully balanced conditions (Kobayashi et al. 2005).

In most of previous works, the fractions of FS energy given to electrons,  $\epsilon_e$ , and to magnetic field,  $\epsilon_B$ , were assumed to be the same as the corresponding fractions in the RS. However, this may not necessary be the case. Fan et al. (2002) performed a detailed fit to the optical flash of GRB 990123 data and obtained  $\epsilon_e^r = 4.7\epsilon_e^f$  and  $\epsilon_B^r = 400\epsilon_B^f$ , where the superscripts “r” and “f” represent RS and FS, respectively. Similar results were obtained by Zhang, Kobayashi & Mészáros (2003), Kumar & Panaitescu (2003), Panaitescu & Kumar (2004), McMahon, Kumar & Panaitescu (2004), and Fan et al. (2005). In this section, we study the RS/FS emission in X-ray band by adopting different shock parameters. We focus on the thin shell case (i.e., the RS is sub-relativistic, see Kobayashi [2000]), in which the RS emission is well separated from the prompt  $\gamma$ -ray emission.

**ISM model.** In the thin shell case, the observer’s time at which RS crosses the ejecta can be estimated by (e.g., Fan et al. 2005)

$$t_\times \approx 128s \left( \frac{1+z}{2} \right) E_{\text{iso},53}^{1/3} n_0^{-1/3} \eta_{2.3}^{-8/3}, \quad (1)$$

where  $E_{\text{iso}}$  is the isotropic energy of the outflow,  $n$  is the typical number density of ISM, and  $\eta$  is the initial Lorentz factor of the outflow. The convention  $Q_y = Q/10^y$  has been adopted in cgs units throughout the text except for some special notations.

In the standard afterglow model of a fireball interacting with a constant density medium (e.g., Sari, Piran & Narayan 1998), the cooling frequency  $\nu_{c,\oplus}^f$ , the typical synchrotron frequency  $\nu_{m,\oplus}^f$ , and the maximum spectral flux  $F_{\nu,\text{max}}^f$  read:  $\nu_{c,\oplus}^f = 4.4 \times 10^{17} \text{ Hz } E_{\text{iso},53}^{-1/2} \epsilon_{B,-3}^{-3/2} n_0^{-1} t_{d,-3}^{-1/2} (\frac{2}{1+z})(1+Y^f)^{-2}$ ,  $\nu_{m,\oplus}^f = 4.4 \times 10^{15} \text{ Hz } E_{\text{iso},53}^{1/2} \epsilon_{B,-3}^{1/2} \epsilon_{e,-1}^{-1} t_{d,-3}^{-3/2} C_p^2 (\frac{2}{1+z})$ , and  $F_{\nu,\text{max}}^f = 2.6 \text{ mJy } E_{\text{iso},53}^{1/2} \epsilon_{B,-3}^{1/2} n_0^{1/2} D_{L,28.34}^{-2} (\frac{1+z}{2})$ , where  $C_p = 13(p-2)/[3(p-1)]$ ,  $p \sim 2.3$  is the typical power-law distribution index of the electrons accelerated by FS,  $Y^f \simeq [-1 + \sqrt{1 + 4x^f \epsilon_e^f / \epsilon_B^f}] / 2$  is the Compton parameter,  $x^f \approx \min\{1, (\nu_m^f / \nu_c^f)^{(p-2)/2}\}$  (Sari & Esin 2001), and  $D_L$  is the luminosity distance for  $(\Omega_M, \Omega_\Lambda, h) = (0.3, 0.7, 0.71)$ . Hereafter  $t = t_\oplus / (1+z)$ , and  $t_d$  is in unit of days.

Following Zhang et al. (2003), we take  $\epsilon_e^r = \mathcal{R}_e \epsilon_e^f$  and  $\epsilon_B^r = \mathcal{R}_B \epsilon_B^f$ . At  $t_\times$ , the RS emission satisfies [See also Fan et al. (2005), note that a novel effect taken into account here is the inverse Compton cooling of the electrons]

$$\nu_{m,\oplus}^r(t_\times) = \mathcal{R}_B [\mathcal{R}_e (\gamma_{34,\times} - 1)]^2 \nu_{m,\oplus}^f(t_\times) / (\Gamma_\times - 1)^2 \quad (2)$$

$$\nu_{c,\oplus}^r(t_\times) \approx \mathcal{R}_B^{-3} [(1+Y^f)/(1+Y^r)]^2 \nu_{c,\oplus}^f(t_\times), \quad (3)$$

$$F_{\nu,\text{max}}^r(t_\times) \approx \eta \mathcal{R}_B F_{\nu,\text{max}}^f(t_\times). \quad (4)$$

where  $\gamma_{34,\times} \approx (\eta/\Gamma_\times + \Gamma_\times/\eta)/2$  is the Lorentz factor of the shocked ejecta relative to the initial one,  $\Gamma_\times$  is the bulk Lorentz factor of the shocked ejecta at  $t_\times$ ,  $Y^r \simeq [-1 + \sqrt{1 + 4x^r \mathcal{R}_e \epsilon_e^f / (\mathcal{R}_B^2 \epsilon_B^f)}] / 2$  is the Compton parameter and  $x^r \approx \min\{1, (\nu_m^r / \nu_c^r)^{(p-2)/2}\}$ .

If both  $\nu_{c,\oplus}^r$  and  $\nu_{m,\oplus}^r$  are below the observed frequency  $\nu_\oplus$ , the detected flux of RS and FS emission are

$$F_{\nu_\oplus}^r(t_\times) \simeq F_{\nu,\text{max}}^r(t_\times) [\nu_{m,\oplus}^r(t_\times)]^{(p-1)/2} [\nu_{c,\oplus}^r(t_\times)]^{1/2} \nu_\oplus^{-p/2}, \quad (5)$$

$$F_{\nu_\oplus}^f(t_\times) \simeq F_{\nu,\text{max}}^f(t_\times) [\nu_{m,\oplus}^f(t_\times)]^{(p-1)/2} [\nu_{c,\oplus}^f(t_\times)]^{1/2} \nu_\oplus^{-p/2}. \quad (6)$$

$$\frac{F_{\nu_\oplus}^r(t_\times)}{F_{\nu_\oplus}^f(t_\times)} \approx \eta \mathcal{R}_B^{\frac{p-2}{2}} \mathcal{R}_e^{p-1} \left( \frac{\gamma_{34,\times} - 1}{\Gamma_\times - 1} \right)^{p-1} \left( \frac{1+Y^f}{1+Y^r} \right). \quad (7)$$

Taking  $p = 2.3$  (such a choice is to match the observed slope of the X-ray flare  $\beta = p/2 = 1.15$ , see P05),  $\Gamma_\times \approx \eta/2 \sim 100$ ,  $\epsilon_{B,-3}^f = 1$ ,  $\epsilon_{e,-1}^f = 1$ ,  $\mathcal{R}_B = 10$  and  $\mathcal{R}_e = 5$ , we have  $x^f \approx 1$ ,  $Y^f \approx (\epsilon_e/\epsilon_B)^{1/2} = 10$ ,  $x^r \approx 0.6$ ,  $Y^r \approx 1.2$ , and  $(1+Y^f)/(1+Y^r) \gg 1$ , i.e., we have a larger contrast  $F_{\nu_\oplus}^r(t_\times)/F_{\nu_\oplus}^f(t_\times)$  when the inverse Compton effect has been taken into account. With equation (7), we have  $F_{\nu_\oplus}^r(t_\times)/F_{\nu_\oplus}^f(t_\times) \approx 5$ , i.e., *in the X-ray band, the RS emission component is dominant*. For  $t_\oplus > t_\times$ , the RS emission declines as  $(t_\oplus/t_\times)^{-(2+p/2)}$  because of the curvature effect (e.g., Kumar & Panaitescu 2000, hereafter KP00)<sup>2</sup>. The FS emission declines as  $t_\oplus^{(2-3p)/4}$  (e.g., Sari et al. 1998), so the X-ray flare lasts  $\sim [F_{\nu_\oplus}^r(t_\times)/F_{\nu_\oplus}^f(t_\times)]^{4/(10-p)} t_\times \sim 300 \text{ s}$ . Taking  $z = 0.36$ ,  $Q_y = 1$ , and  $\nu_\times = 2.4 \times 10^{17} \text{ Hz}$ , we have  $\nu_\times F_{\nu_\times}^f \sim 10^{-9} \text{ ergs cm}^{-2} \text{ s}^{-1} [(1+z)/1.36] D_{L,27.7}^{-2}$ . The peak flux of the X-ray flare is  $\simeq \nu_\times [F_{\nu_\times}^f + F_{\nu_\times}^r] \sim 5 \times 10^{-9} \text{ ergs cm}^{-2} \text{ s}^{-1} [(1+z)/1.36] D_{L,27.7}^{-2}$ , which is consistent with the observation of GRB 011121 ( $\sim 2.4 \times 10^{-9} \text{ ergs cm}^{-2} \text{ s}^{-1}$ , see P05). However, the accompanying optical flash is very bright. With the typical parameters taken here, the V band flux is  $\sim 5 \text{ Jy}$ .

**Wind model.** GRB 011121 was born in a stellar wind. The best fit parameters are  $p = 2.5$ ,  $E_{\text{iso},52} = 2.8$ ,  $A_* \sim 0.003$ ,  $\epsilon_e^f \sim 0.01$ , and  $\epsilon_B^f \sim 0.5$  (P05). It is straightforward to show that with proper choice of  $\mathcal{R}_e$  and  $\mathcal{R}_B$ , at  $t_\times$ , the RS emission may be dominant in the soft X-ray band.

**Numerical results.** Following Fan et al. (2005), the FS-RS emission (in the X-ray band) has been calculated numerically. In the ISM case (see Fig. 1(a)), the parameters are taken as  $E_{\text{iso},53} = 1$ ,  $p = 2.4$ ,  $\epsilon_e^f = 0.1$ ,  $\epsilon_B^f = 0.001$ ,  $n = 1 \text{ cm}^{-3}$ , and the initial width of the outflow  $\Delta = 6 \times 10^{11} \text{ cm}$ . In the wind case (see Fig. 1(b)), we take the best fit parameters presented in P05.

As shown in Fig. 1(a), in the ISM case, there comes an X-ray flare dominated by the RS emission only when both  $\mathcal{R}_B$  and  $\mathcal{R}_e$  are much larger than unity. In the wind case, with proper  $\mathcal{R}_B$  and  $\mathcal{R}_e$ , the RS emission may be dominant in the soft X-ray band, too. But there is no flare expected since both the FS and RS emission components decrease continually even at very early time (see also Zou, Wu & Dai 2005). So the FS-RS scenario is unable to account for the X-ray flare detected in GRB 011121. Moreover, in the general framework of accounting for X-ray flares in GRB afterglows, the FS-RS model is further disfavored for the fact that, even in an ISM scenario with parameters suitable for a RS flare arising above the FS emission, the predicted temporal decay

<sup>2</sup> To derive the curvature effect, two assumptions are made (KP00). One is that the Lorentz factor of the outflow is nearly a constant. The other is that the observer frequency should be above the cooling frequency of the emission. As far as the reverse shock emission mentioned here, these assumptions are satisfied. So we take  $(t_\oplus/t_\times)^{-(2+p/2)}$  to describe the decline, which has been verified by the detailed numerical calculation (Fan, Wei & Wang 2004; see also Fig. 1 of this work).

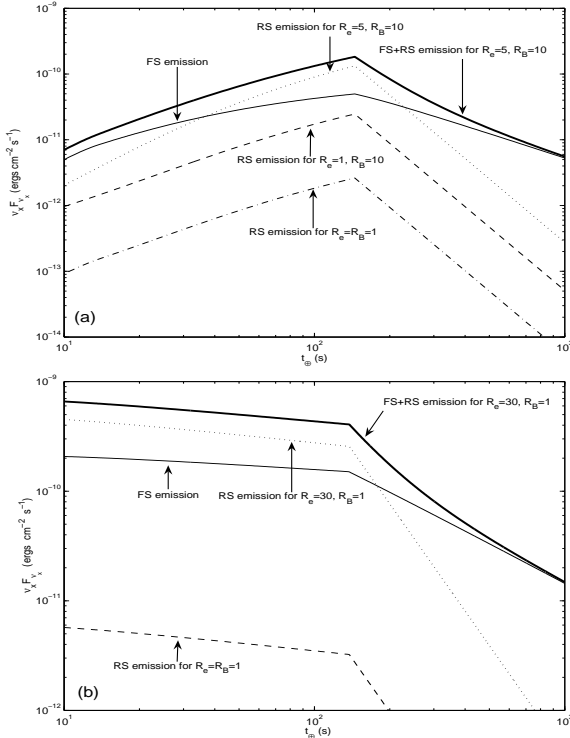


**Figure 1.** The very early X-ray ( $\nu_x = 2.42 \times 10^{17}$  Hz) sample lightcurves. For the reverse shock emission component,  $\mathcal{R}_e$  and  $\mathcal{R}_B$  have been marked in the figure. (a) The ISM case, the parameters are taken as  $n = 1 \text{ cm}^{-3}$ ,  $E_{\text{iso},53} = 1$ ,  $z = 1$ ,  $\Delta = 6 \times 10^{11} \text{ cm}$ ,  $\epsilon_e^f = 0.1$ ,  $\epsilon_B^f = 0.001$ ,  $\eta = 200$ , and  $p = 2.4$ . (b) The wind case, following P05, we take  $A_* = 0.003$ ,  $\epsilon_e^f = 0.01$ ,  $\epsilon_B^f = 0.5$ ,  $E_{\text{iso},53} = 0.28$ ,  $p = 2.5$ , and  $z = 0.36$ ; In addition, we assume  $\eta = 200$  and  $\Delta = 3.0 \times 10^{12} \text{ cm}$ .

is too shallow compared to the steep decay of X-ray flares observed so far (see Fig. 1).

## 2.2 Late internal shock model

In the standard fireball model of GRBs, the  $\gamma$ -ray emission is powered by internal shocks, whose duration depends on the active time of the central engine. However, the variability of some GRB afterglows implies that the activity of the GRB central engine may last much longer than the duration of the prompt emission recorded by  $\gamma$ -ray monitors (e.g., Dai & Lu 1998; Granot, Nakar & Piran 2003; Ioka, Kobayashi & Zhang 2005). In addition, it has been proposed that the Fe line observed in some GRB X-ray afterglows could be attributed to a prolonged activity of the central engine (Rees & Mészáros 2000; Gao & Wei 2005).

A possible mechanism for the re-activity of the central engine could be as follows. During the accretion phase which powers the prompt  $\gamma$ -ray emission, a fraction of the material constituting the massive progenitor could possibly be pulled out; the central engine could thus be restarted at late times by the fall back of part of this material onto the central collapsar remnant (King et al. 2005).

Here we assume that the central engine restarts a few minutes after the prompt  $\gamma$ -ray emission, powering a new

unsteady relativistic outflow. We suppose that the Lorentz factor of the ejected material can be highly variable, setting  $\Gamma_s \sim 10$  and  $\Gamma_f \sim 100$ , as the typical Lorentz factors of the slow and fast shells, respectively. The masses of the slow and fast shells are taken as  $m_f \simeq m_s$ . When an inner fast shell catches up with an outer slow shell at a radius  $\sim 2\Gamma_s^2 c \delta t_{\oplus} / (1+z)$  (where  $\delta t_{\oplus}$  is the observed typical variability timescale of the X-ray flares), internal shocks are generated. The Lorentz factor of the merged shell is  $\Gamma \approx \sqrt{\Gamma_f \Gamma_s}$  (e.g., Piran 1999), and the Lorentz factor of the internal shocks can be estimated by  $\Gamma_{\text{sh}} \approx (\sqrt{\Gamma_f/\Gamma_s} + \sqrt{\Gamma_s/\Gamma_f})/2$ . We call this re-generated internal shocks as the “late internal shocks”.

### 2.2.1 Physical parameters

The internal shock model has been discussed by many authors (e.g., Paczyński & Xu 1994; Rees & Mészáros 1994; Daigne & Mochkovitch 1998, 2000; Piran 1999; Dai & Lu 2002). Generally speaking, to calculate the synchrotron emission of internal shocks, the following parameters are involved: the outflow luminosity  $L_m$ ,  $\delta t_{\oplus}$ ,  $\Gamma$ ,  $\Gamma_{\text{sh}}$ , and of course the shock parameters  $\epsilon_e$  and  $\epsilon_B$ . For typical GRBs, ( $L_m$ ,  $\delta t_{\oplus}$ ,  $\Gamma$ ,  $\Gamma_{\text{sh}}$ ,  $\epsilon_e$ ,  $\epsilon_B$ ) are taken to be  $\sim (10^{52} \text{ ergs s}^{-1}, 0.001-0.01 \text{ s}, 100-1000, \text{ a few}, 0.5, 0.01-0.1)$ , respectively (e.g., Dai & Lu 2002).

The time averaged isotropic luminosity (2-700 keV) of the X-ray re-bursting of GRB 011121 is  $L_x \sim 6 \times 10^{48} \text{ ergs s}^{-1}$  (P05). So we normalize our expression by taking  $L_m \sim 5 \times 10^{49} L_{x,49} (\epsilon/0.2)^{-1} \text{ ergs s}^{-1}$ , where  $\epsilon$  is the efficiency factor of the X-ray flare. We take  $\epsilon \sim 0.2$ , as found in typical GRBs/XRFs (Lloyd-Ronning & Zhang 2004). Such small  $L_m$  (comparing with the GRB case) implies that the fallback accretion rate is just  $\sim 0.001-0.01$  times that of the prompt accretion, if the efficiency factor of converting the accretion energy into the kinetic energy of the outflow is nearly a constant (MacFadyen, Woosley & Heger 2001).

The  $\delta t_{\oplus}$  measured in X-ray flares is significantly longer than that measured in the intrinsic hard burst (Burrows et al. 2005). In this Letter, we take  $\delta t_{\oplus} \sim 10 \text{ s}$ . The spectra of the X-ray flares detected so far are all nonthermal. The optical thin condition implies a lower limit on the bulk Lorentz factor of the merged shell (e.g., Rees & Mészáros 1994)

$$\Gamma > 11 L_{m,49.7}^{1/5} [1.36/(1+z)]^{-1/5} \delta t_{\oplus,1}^{-1/5}, \quad (8)$$

The typical radius of the late internal shock is  $R_{\text{int}} \approx 2\Gamma^2 c \delta t_{\oplus} / (1+z) > 5 \times 10^{13} \text{ cm } L_{m,49.7}^{2/5} [1.36/(1+z)]^{3/5} \delta t_{\oplus,1}^{3/5}$ .

As we will show in the following section, with  $L_m \sim 5 \times 10^{49} \text{ ergs s}^{-1}$ ,  $\delta t_{\oplus} \sim 10 \text{ s}$ ,  $\Gamma \sim 30$ ,  $\Gamma_{\text{sh}} \sim 2$ ,  $\epsilon_e \sim 0.5$ , and  $\epsilon_B \sim 0.1$ , most of the internal shocks energy is emitted in the soft X-ray band and the predicted flux matches the observation of the X-ray flare in GRB 011121. Alternatively, as shown in Barraud et al. (2005), with  $\epsilon \sim 0.01$  (correspondingly,  $L_m \sim 10^{51} - 10^{52} \text{ ergs s}^{-1}$  and  $\Gamma_{\text{sh}} \sim 1.06$ ),  $\delta t_{\oplus} \sim$  a few seconds, and  $\Gamma \sim$  a few hundreds, X-ray dominated luminosity is expected, too (Please note that their calculation of the internal shocks emission is somewhat different from ours; see Barraud et al. 2005 for detail). Therefore, we believe that with proper parameters, X-ray flares do appear in the late internal shocks scenario.

### 2.2.2 The synchrotron radiation of the “late internal shocks”

Following Dai & Lu (2002), the comoving number density of the unshocked outflow is estimated by  $n_e \approx L_m / (4\pi\Gamma^2 R_{\text{int}}^2 m_p c^3)$ , where  $m_p$  is the rest mass of proton. The thermal energy density of the shocked material is calculated by  $e \approx 4\Gamma_{\text{sh}}(\Gamma_{\text{sh}} - 1)n_e m_p c^2$  (Blandford & McKee 1977). The intensity of the generated magnetic field is estimated by  $B \approx (8\pi\epsilon_B e)^{1/2} \approx 6 \times 10^3 \text{ G } \epsilon_{B,-1}^{1/2} [\Gamma_{\text{sh}}(\Gamma_{\text{sh}} - 1)/2]^{1/2} L_{m,49.7}^{1/2} \Gamma_{1.5}^{-1} R_{\text{int},14.5}^{-1}$ .

As usual, we assume that in the shock front, the accelerated electrons distribute as  $dn_e/d\gamma_e \propto \gamma_e^{-p}$  for  $\gamma_e > \gamma_{e,m}$ , where  $\gamma_{e,m} = \epsilon_e(\Gamma_{\text{sh}} - 1)[(p-2)m_p]/[(p-1)m_e]$  is the minimum Lorentz factor of the shocked electrons (Sari et al. 1998), and  $m_e$  is the rest mass of electron. In this section, we take  $p=2.5$ . The observed typical frequency of the synchrotron radiation reads

$$\begin{aligned} \nu_{m,\oplus} &= \gamma_{e,m}^2 q_e \Gamma B / [2(1+z)\pi m_e c] \\ &\simeq 2.7 \times 10^{16} \text{ Hz } \epsilon_{e,-0.3}^2 \epsilon_{B,-1}^{1/2} (\Gamma_{\text{sh}} - 1)^{5/2} (\Gamma_{\text{sh}}/2)^{1/2} \\ &\quad L_{m,49.7}^{1/2} \Gamma_{1.5}^{-2} \delta t_{\oplus,1}^{-1}, \end{aligned} \quad (9)$$

i.e., most of the shock energy is emitted in the soft X-ray band, where  $q_e$  is the charge of electron.

The cooling Lorentz factor is estimated by (e.g., Sari et al. 1998)  $\gamma_{e,c} \approx 7.7 \times 10^8 (1+z)/(\Gamma B^2 \delta t_{\oplus})$ , and the corresponding cooling frequency reads

$$\begin{aligned} \nu_{c,\oplus} &= \gamma_{e,c}^2 q_e \Gamma B / [2(1+z)\pi m_e c] \\ &\simeq 10^{10} \text{ Hz } [1.36/(1+z)]^2 \epsilon_{B,-1}^{-3/2} \Gamma_{1.5}^8 \\ &\quad [\Gamma_{\text{sh}}(\Gamma_{\text{sh}} - 1)/2]^{-3/2} L_{m,49.7}^{-3/2} \delta t_{\oplus,1}. \end{aligned} \quad (10)$$

The synchrotron self-absorption frequency is estimated by (Li & Song 2004)

$$\nu_{a,\oplus} \simeq 10^{15} \text{ Hz } [1.36/(1+z)]^{3/7} L_{m,49.7}^{2/7} \Gamma_{1.5}^{-5/7} \delta t_{\oplus,1}^{-4/7} B_3^{1/7}. \quad (11)$$

The maximum spectral flux of the synchrotron radiation is (e.g., Wijers & Galama 1999)  $F_{\text{max}} \approx 3\sqrt{3}\Phi_p(1+z)N_e m_e c^2 \sigma_T \Gamma B / (32\pi^2 q_e D_L^2)$ , where  $N_e = L_m \delta t / [(1+z)\Gamma m_p c^2] = 8 \times 10^{51} [1.36/(1+z)] L_{m,49.7} \Gamma_{1.5}^{-1} \delta t_{\oplus,1}$  is the number of electrons involved in the emission.  $\Phi_p$  is a function of  $p$ , for  $p = 2.5$ ,  $\Phi_p \approx 0.6$  (Wijers & Galama 1999). For  $\nu_{c,\oplus} < \nu_{a,\oplus} < \nu_x < \nu_{m,\oplus}$ , the predicted flux is (e.g., Sari et al. 1998)

$$\begin{aligned} F_{\nu_x} &= F_{\text{max}}(\nu_{m,\oplus}/\nu_{c,\oplus})^{-1/2} (\nu_x/\nu_{m,\oplus})^{-p/2} \\ &\approx 2.5 \text{ mJy } [\nu_x/(2.42 \times 10^{17} \text{ Hz})]^{-p/2} \epsilon_{e,-0.3}^{p-1} \epsilon_{B,-1}^{(p-2)/4} \\ &\quad (\Gamma_{\text{sh}}/2)^{(p-2)/4} (\Gamma_{\text{sh}} - 1)^{(5p-6)/4} L_{m,49.7}^{(p+2)/4} \\ &\quad \Gamma_{1.5}^{2-p} \delta t_{\oplus,1}^{(2-p)/2} D_{L,27.7}^{-2}. \end{aligned} \quad (12)$$

Taking  $Q_y = 1$  and  $\nu_x = 2.42 \times 10^{17} \text{ Hz}$ , with equation (12) we have  $F_{\nu_x} \approx 2.5 \text{ mJy}$ , which matches the observation of GRB 011121 ( $\sim 1 \text{ mJy}$ ). The V band flux can be estimated as ( $\nu_{c,\oplus} < \nu_v < \nu_{a,\oplus}$ )  $F_{\nu_v} \sim F_{\text{max}} \nu_{a,\oplus}^{-3} \nu_{c,\oplus}^{1/2} \nu_v^{5/2} \sim 40 \text{ mJy}$ .

What happens after the “late internal shocks”? Surely, the refreshed relativistic outflow will catch up with the initial outflow when the latter has swept a large amount of material and got decelerated. That energy injection would give rise to a flattening (e.g., Rees & Mészáros 1998) or re-brightening signature (e.g., Panaitescu, Mészáros & Rees

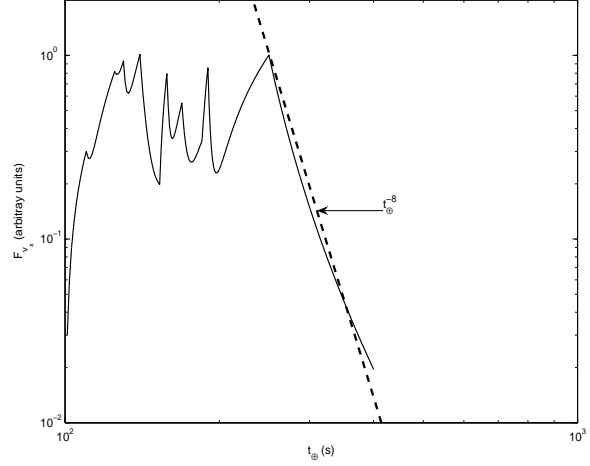


**Figure 2.** The X-ray lightcurve of one flare consisting of ten pulses (the solid line, for illustration), each takes the profile  $F_{\nu_x} \propto [(t_{\oplus} - t_{\text{eje}})/\delta t_{\oplus}]$  for  $t_{\oplus} < t_{\text{eje}} + \delta t_{\oplus}$  and  $F_{\nu_x} \propto [(t_{\oplus} - t_{\text{eje}})/\delta t_{\oplus}]^{-3.25}$  for  $t_{\oplus} > t_{\text{eje}} + \delta t_{\oplus}$ . In these pulses ( $i = 1 - 10$ ), the peak of  $F_{\nu_x,i}$  are taken to be (0.3, 0.8, 0.6, 0.9, 0.1, 0.7, 0.5, 0.3, 0.7, 1.0), respectively (in arbitrary units);  $\delta t_{\oplus,i}$  are taken to be (10, 15, 5, 10, 13, 5, 9, 11, 5, 60) s, respectively;  $t_{\text{eje},i}$  are taken to be (100, 110, 125, 130, 140, 153, 158, 169, 185, 190) s, respectively.  $t_{e,\oplus} \approx t_{\text{eje},10} + \delta t_{\oplus,10} = 250 \text{ s}$ . The dashed line represents  $F_{\nu_x} \propto (t_{\oplus}/t_{e,\oplus})^{-8}$ .

1998; Kumar & Piran 2000; Zhang & Mészáros 2002), which could potentially account for the late re-brightening of XRF 050406, the late X-ray re-bursting detected in GRB 050502b and the second/weaker X-ray bump observed in GRB 011121. However, the detailed lightcurve modeling is beyond the scope of this Letter.

### 2.2.3 The decline behavior of the flare

For observer’s frequencies above the cooling frequency, the curvature effect dominates the temporal behavior of the observed flux after the central engine shuts down at  $t_{e,\oplus}$  (PK00). The flux declines as  $\sum_i F_{\nu_x,i} [(t_{\oplus} - t_{\text{eje},i})/\delta t_{\oplus,i}]^{-(2+p_i/2)}$  (PK00), where  $i$  represents the  $i$ th pulse,  $t_{\text{eje},i}$  and  $t_{\oplus,i}$  are the ejection time and the variability timescale of the  $i$ th pulse, respectively. Such a decline is much steeper than  $(t_{\oplus}/t_{e,\oplus})^{-(2+p/2)}$  for  $t_{e,\oplus} \gg \max\{\delta t_{\oplus,i}\}$ . For example, as shown in Fig. 2, the decline of the flare is dominated by the curvature effect of the last long pulse with  $\delta t_{\oplus} \sim 0.24 t_{e,\oplus}$ . A crude power-law fit to the decline yields  $F_{\nu_x} \propto (t_{\oplus}/t_{e,\oplus})^{-8}$ , which is steep enough to match the sharpest decline detected so far. In reality, the central engine does not turn off abruptly. The dimmer and dimmer emission powered by the weaker and weaker “late internal shocks” may dominate over the curvature effect of the early pulses, resulting in a shallower decay.

### 3 DECLINE BEHAVIOR OF THE X-RAY FLARE: CONSTRAINT ON THE MODEL

Early X-ray flares have been well detected in GRB 011121, XRF 050406, GRB 050502b and GRB 050730 (P05; Burrows et al. 2005; Starling et al. 2005). The rise and fall of the first flare (also the dominant one) in GRB 011121 are both very steep. Similar temporal behavior is evident in other events. The sharp decline of these flares imposes a robust constraint on the model, as shown below.

The X-ray flare detected in GRB 011121 appears at  $t_{b,\oplus} = 239$  s and peaks at  $t_{p,\oplus} = 270$  s. The burst is believed to be born in a weak stellar wind. As shown in Fig. 1(b), no flare is expected in the FS-RS model. The FS-RS shock model is further disfavored by its shallow decline. In the late internal shock model, the decline of the flare can be steep enough to account for the observation (see Fig. 2 for illustration). Moreover, as shown in §2.2.2, with proper parameters the observed flux can be well reproduced. So the “late internal shock model” is favored. We would like to point out that *the fall of the X-ray flare detected in GRB 011121 is still attributed to the late internal shocks rather than the curvature effect*. The reason is as follows. Since  $\delta t_{\oplus} \leq (t_{p,\oplus} - t_{b,\oplus}) = 31$  s, the resulted decline  $F_{\nu_x} \propto [1 + (t_{\oplus} - 270)/\delta t_{\oplus}]^{-3.15}$  is much steeper than the observation  $F_{\nu_x} \propto [(t_{\oplus} - 239)/31]^{-1.4}$  (see Fig. 7 of P05) if after  $t_{p,\oplus}$  there are no internal shocks any more.

The X-ray flare detected in XRF 050406 peaks at  $t_{p,\oplus} \approx 210$  s and declines as  $F \propto t_{\oplus}^{-5.7}$ . The X-ray flare detected in GRB 050502b peaks at  $t_{p,\oplus} \approx 650$  s and declines as  $F \propto t_{\oplus}^{-7}$ . In the X-ray afterglow lightcurve of GRB 050730, there are three X-ray flares (ranging from 200 s to 800 s after the trigger of the GRB). A crude fit to the decline of these three flares results in  $F \propto t_{\oplus}^{-5}$  or steeper. Obviously, the FS-RS scenario is ruled out by the steep observed decays and the “late internal shock model” is favored. For the X-ray flare detected in GRB 050502b, the late internal shock model interpretation is further supported by the sharp spike detected in 1.0–10.0 keV band (Burrows et al. 2005).

### 4 SUMMARY & DISCUSSION

In this work, we have explored two possible models which might give rise to X-ray flares in GRB afterglows. One is the external forward-reverse shock model (the ISM case), in which the shock parameters of forward/reverse shocks are taken to be quite different. *The other is the “late internal shock model”, which requires that a refreshed unsteady relativistic outflow is generated after the prompt  $\gamma$ -ray emission* (see Ramirez-Ruiz, Merloni & Rees [2001] for alternative scenarios), *perhaps due to the fallback accretion onto the central collapsar remnant*. The refreshed outflow may be characterized by a low outflow luminosity ( $\sim 10^{49}$  ergs s $^{-1}$ ), a small bulk Lorentz factor ( $\sim 30$ ), and a long variability timescale ( $\sim 10$  s). In the external forward-reverse shock model, after the peak of the reverse shock emission ( $t_{p,\oplus} = t_x$ ), the flux can not decline more sharply than  $(t_{\oplus}/t_{p,\oplus})^{-(2+p/2)}$  (see Fig. 1 for illustration). In the “late internal shock model”, the decline can be much steeper than  $(t_{\oplus}/t_{e,\oplus})^{-(2+p/2)}$  if the central engine shuts down after  $t_{e,\oplus}$  and the longest variability timescale of the X-ray flare is much shorter than  $t_{e,\oplus}$  (see Fig. 2 for illustration).

For the X-ray flares detected in GRB 011121, XRF 050406, GRB 050502b and GRB 050730, the external forward-reverse shock model is ruled out directly by its shallow temporal decay. For the same reason, other possible external models (i.e., the model related to the external forward shock), including the density jump model, the two-components jet model, the patch jet model as well as the energy injection model are ruled out too (Zhang et al. 2005). Thus, the “late internal shock model” is found to be favored. In this model, the optical emission may be suppressed due to strong synchrotron-self-absorption. But in the ultraviolet band, the radiation could be quite strong. Large amount of neutral gas would be ionized, as detected in GRB 050502b and GRB 050730 (Burrows et al. 2005; Starling et al. 2005).

*Very early X-ray flares are well detected both in long GRBs and in XRFs, which strengthens the correlation of these two phenomena*, though the nature of XRFs is still unclear (Barraud et al. 2005 and the references therein).

Finally, we suggest that the early X-ray light curve of some GRBs may be a superposition of the emission powered by the long activity of the central engine and the emission of the external forward shock. As a consequence, the X-ray temporal behavior may be quite different from that of the long wavelength emission (UV/Optical ones). This prediction can be tested by the UVOT and XRT on board *Swift* observatory directly in the near future.

### ACKNOWLEDGMENTS

We thank Bing Zhang and E. W. Liang for informing us Piro et al.’s paper on GRB 011121 at the end of Feb, and G. F. Jiang, L. J. Gou, Z. Li and H. T. Ma for kind help. We also appreciate the referees for their helpful comments and the third referee for her/his great help. This work is supported by the National Natural Science Foundation (grants 10225314 and 10233010) of China, and the National 973 Project on Fundamental Researches of China (NKBRSF G19990754).

### REFERENCES

- Akerlof C. et al. 1999, *Nature*, 398, 400
- Barraud C., Daigne F., Mochkovitch R., Atteia J. L. 2005, *A&A*, in press (astro-ph/0507173)
- Blandford, R. D., & McKee, C. F. 1977, *MNRAS*, 180, 343
- Blake C. H. et al. 2005, *Nature*, 435, 181
- Bloom J. S., et al. 2002, *ApJ*, 572, L45
- Burrows, D. N., et al. 2005, *Science*, in press (astro-ph/0506130)
- Dai Z. G., Lu T., 1998, *A&A*, 333, L87
- Dai Z. G., Lu T., 2002, *ApJ*, 580, 1013
- Daigne F., Mochkovitch R. 1998, *MNRAS*, 296, 275
- Daigne F., Mochkovitch R. 2000, *A&A*, 358, 1157
- Fan Y. Z., Dai Z. G., Huang Y. F., Lu T., 2002, *Chin. J. Astron. Astrophys.* 2, 449 (astro-ph/0306024)
- Fan Y. Z., Wei D. M., Wang C. F., 2004, *A&A*, 424, 477
- Fan Y. Z., Zhang B., Wei D. M., 2005, *ApJ*, 628, L25
- Fox D. et al. 2003, *ApJ*, 586, L5
- Gao W. H., Wei D. M., 2005, *ApJ*, 628, 853
- Garnavich P. M., et al. 2003, *ApJ*, 582, 924
- Granot J., Nakar E., Piran T., 2003, *Nature*, 426, 138
- Greiner J., et al. 2003, *ApJ*, 599, 1223

- Infante L., Garnavich P. M., Stanek K. Z., Wyrzykowski L., 2001, GCN Circ., 1152
- Ioka K., Kobayashi S., Zhang B., 2005, ApJ, in press (astro-ph/0409376)
- King A., O'Brien P. T., Goad M. R., Osborne J., Olsson E., Page K. 2005, ApJL, in press (astro-ph/0508126)
- Kobayashi S. 2000, ApJ, 545, 807
- Kobayashi S., Zhang B., Mészáros P., Burrows W., 2005, ApJL, submitted (astro-ph/0506157)
- Kumar P., Panaitescu A., 2003, MNRAS, 346, 905
- Kumar P., Panaitescu A., 2000, ApJ, 541, L51 (KP00)
- Kumar P., Piran T., 2000, ApJ, 532, 286
- Li Z., Song L. M. 2004, ApJ, 608, L17
- Li W. D., Filippenko A. V., Chornock R., Jha S., 2003, ApJ, 586, L9
- Lloyd-Ronning, N. M., & Zhang, B. 2004, ApJ, 601, 371
- MacFadyen A. I., Woosley S. E., Herger A. 2001, ApJ, 550, 410
- McMahon E., Kumar P., Panaitescu A., 2004, MNRAS, 354, 915
- Mészáros P., Rees M. J., 1999, MNRAS, 306, L39
- Paczynski B., Xu G. H., 1994, ApJ, 427, 708
- Panaitescu A., Kumar P., 2004, MNRAS, 353, 511
- Panaitescu A., Mészáros P., Rees M. J., 1998, ApJ, 503, 314
- Piran T., 1999, Phys. Rep., 314, 575
- Piro L., 2001, GCN Circ. 1147
- Piro L. et al., 2005, ApJ, 623, 314 (P05)
- Price P. A., et al. 2002, ApJ, 572, L51
- Ramirez-Ruiz E., Merloni A., Rees M. J., 2001, MNRAS, 324, 1147
- Rees M. J., Mészáros P., 1994, ApJ, 430, L93
- Rees M. J., Mészáros P., 1998, ApJ, 496, L1
- Rees M. J., Mészáros P., 2000, ApJ, 545, L73
- Sari R., Esin A. A. 2001, ApJ, 548, 787
- Sari R., Piran T. 1999, ApJ, 517, L109
- Sari R., Piran T., Narayan R. 1998, ApJ, 497, L17
- Starling R. L. C., et al. 2005, A&A, submitted (astro-ph/0508237)
- Wang X. Y., Dai Z. G., Lu T., 2001, ApJ, 556, 1010
- Wei D. M. 2003, A&A, 402, L9
- Wijers R. A. M. J., & Galama T. J. 1999, ApJ, 523, 177
- Zhang B., Fan Y. Z., Dyks J., Kobayashi S., Mészáros P., Burrows D. N., Nousek J. A., Gehrels N. 2005, ApJ, submitted (astro-ph/0508321)
- Zhang B., Kobayashi S., Mészáros P., 2003, ApJ, 595, 950
- Zhang B., Mészáros P., 2002, ApJ, 566, 712
- Zou Y. C., Wu X. F., Dai Z. G., 2005, MNRAS, in press (astro-ph/0508602)

## APPENDIX A: DERIVATION OF THE CURVATURE EFFECT

Assuming a shell is ejected at  $t_{\text{eje}}$  and moves with a constant Lorentz factor  $\Gamma$  (the corresponding velocity is  $V$ , in unit of the speed of light), the electrons are shock-accelerated at  $R < R_{\text{cro}}$  and cools rapidly, where  $R_{\text{cro}}$  is the radius after which there is no newly relativistic electrons injected. For  $R > R_{\text{cro}}$ , the radiation nearly cuts off as long as the observer frequency  $\nu_{\oplus}$  is above the cooling frequency of the electrons. For  $t_{\oplus} > t_0 \equiv t_{\text{eje}} + (1+z)R_{\text{cro}}/(2\Gamma^2 c)$ , the flux received from the shell is given by

$$F_{\nu_{\oplus}}(t_{\oplus}) \propto \int_{\theta_t}^{\theta_j} \frac{\mathcal{S}_{\nu'} \sin \theta d\theta}{\Gamma^3 (1 - V \cos \theta)^3}, \quad (\text{A1})$$

where  $\theta_t$  satisfies  $R_{\text{cro}} \approx c(t_{\oplus} - t_{\text{eje}})/[(1+z)(1 - V \cos \theta_t)]$ ,  $\theta_j$  is the half opening angle of the shell,  $\nu' = \Gamma(1 - V \cos \theta)\nu_{\oplus}$ ,  $\mathcal{S}_{\nu'} \propto (R/R_{\text{cro}})^k \nu'^{-\beta}$  is the specific spectrum of the radiation in unit of solid angle. On the “equal arriving time sur-

face”  $R(\theta) = c(t_{\oplus} - t_{\text{eje}})/[(1+z)(1 - V \cos \theta)]$  (Rees 1966, Nature, 211, 468), the magnetic field, the typical emission frequency of the electrons, and the number of electrons involved in the radiation are all functions of  $R$ , that's why we take into account the term  $(R/R_{\text{cro}})^k$  in calculating  $\mathcal{S}_{\nu'}$ .

Equation (A1) yields

$$\begin{aligned} F_{\nu(t_{\oplus})} &\propto \int_{\theta_t}^{\theta_j} (1 - V \cos \theta_t)^k (1 - V \cos \theta)^{-(3+\beta+k)} \sin \theta d\theta \\ &\approx \frac{1}{2 + \beta + k} (1 - V \cos \theta_t)^{-(2+\beta)}. \end{aligned} \quad (\text{A2})$$

On the other hand,  $F_{\nu(t_0)} \propto \frac{1}{2+\beta+k} (1 - V)^{-(2+\beta)}$ . For  $t_0 < t_{\oplus} < t_j$ , we have

$$F_{\nu(t_{\oplus})} = F_{\nu(t_0)} \left[ \frac{1 - V \cos \theta_t}{1 - V} \right]^{-(2+\beta)} \propto \left( \frac{t_{\oplus} - t_{\text{eje}}}{t_0 - t_{\text{eje}}} \right)^{-(2+\beta)}, \quad (\text{A3})$$

which coincides with that presented in KP00 but derived in a different way.<sup>3</sup>

<sup>3</sup> The derivation of the curvature effect has not been presented in the paper to match the page limit.